

Gina Kaysan¹
Burkard Spiegel¹
Gisela Guthausen²
Matthias Kind^{1,*}

Influence of Shear Flow on the Crystallization of Organic Melt Emulsions – A Rheo-Nuclear Magnetic Resonance Investigation

There is a need to better understand the influence of shear flow on the crystallization of a molten oil phase in an oil/water emulsion due to its high relevance for industrial processes. The present study focuses on the influence of laminar shear flow on the crystallization kinetics of polydisperse *n*-hexadecane-in-water emulsions. The investigation was carried out by rheo-nuclear magnetic resonance (NMR) spectroscopy in a Taylor-Couette geometry. An accelerating impact of the shear rate on the overall crystallization kinetics was verified. This effect stems from an increase of the collision frequency of already crystallized droplets with not yet crystallized droplets. Nevertheless, the collision efficiency decreased with higher shear rate.

Keywords: Couette flow, Crystallization, Organic melt emulsion, Rheo-nuclear magnetic resonance, Shear rate

Received: April 20, 2020; *accepted:* May 05, 2020

DOI: 10.1002/ceat.202000193

 This is an open access article under the terms of the Creative Commons Attribution License, which permits use, distribution and reproduction in any medium, provided the original work is properly cited.



Supporting Information
available online

1 Introduction

1.1 Emulsion Crystallization

Melt emulsions are produced and often also stored under the influence of a flow field during industrial processes, e.g., in the chemical, pharmaceutical, and life science industry [1–3]. Such a flow field and particularly its shear rates lead to interactions and collisions of liquid droplets with already crystallized particles. In-depth understanding of interactions and of the impact of collisions on crystallization provides opportunities for a better control of industrial processes and the product quality produced. It is well-known that crystallization of such droplets is highly statistical and exhibits peculiar behavior which ought to be controlled better. The effect described by these interactions can easily happen because not all the emulsions' droplets crystallize at the same time [4]. The crystallization process of droplets differs from the crystallization of the bulk phase and high subcoolings are needed to achieve high crystal fractions. It is of great interest to investigate the possibility of collision-induced nucleation to increase the fraction of crystallized droplets of emulsions without extending the process time or decreasing the temperature, due to the less energy amount needed.

The influencing parameters should be well defined and considered individually as the number of crystallized droplets after the crystallization process depends on the nucleation rate and colloidal processes [3, 5–8]. Furthermore, the number of solid particles depends on parameters such as the cooling rate and the subcooling [3, 9].

1.2 Collision-Induced Nucleation

A distinction is made in the literature between primary and secondary nucleation mechanisms. The former mechanism is subdivided into homogeneous and heterogeneous nucleation. Homogeneous nucleation takes place when crystal nuclei are formed by virtue of supersaturation alone [10]. Heterogeneous nucleation describes nucleation catalyzed by an active nucleation center. The latter has a different chemical structure than the medium to be crystallized. Plenty of work exists dealing with the influence of primary nucleation on the crystallization of emulsions [3, 9, 11].

Secondary nucleation occurs when crystals are already present in a subcooled melt and catalyze nucleation. This happens due to effects such as attrition caused by mechanical stress, collision, or impact. The chemical structure of the nucleating agent is the same as that of the crystallizing material. Collision-induced nucleation of emulsion droplets is understood as a secondary nucleation mechanism. It is thermodynamically more

¹Gina Kaysan, Dr.-Ing. Burkard Spiegel, Prof. Dr.-Ing. Matthias Kind
matthias.kind@kit.edu

Karlsruhe Institute of Technology, Institute for Thermal Process Engineering, Kaiserstrasse 12, 76131 Karlsruhe, Germany.

²Prof. Dr. Gisela Guthausen

Karlsruhe Institute of Technology, Institute for Mechanical Process Engineering and Mechanics and Engler Bunte Institute Water Chemistry and Technology, Kaiserstrasse 12, 76131 Karlsruhe, Germany.

favorable that nuclei form by such secondary mechanisms than by primary mechanisms. A lower barrier in free energy must be surmounted for the formation of stable crystal nuclei for the homogeneous mechanism than for heterogeneous or secondary nucleation to take place. Therefore, heterogeneous or secondary nucleation, in comparison to homogeneous nucleation, needs less subcooling.

Three different collision mechanisms are discussed in the case of emulsions (Fig. 1) which could lead to collisions and consequently to collision-induced crystallization of droplets [12]:

- perikinetic collisions: caused by a random movement of droplets due to Brownian motion (especially relevant for droplets smaller than $1\ \mu\text{m}$),
- orthokinetic collisions generated by an external velocity gradient, and
- differential collisions: due to different creaming velocities of the colliding droplets (important for droplets bigger than $10\ \mu\text{m}$).

1.3 Influence of Shear Rate

Several mathematical models for predicting the collision rate of liquid droplets can be found in literature. Most of them consider the influence of Brownian motion (Fig. 1a) [13–15]. Only a few authors evaluate the impact of external forces on the crystallization kinetics (Fig. 1b) [4, 9, 16].

McClements et al. [14] hypothesized that crystallization in subcooled liquid droplets for a non-sheared *n*-hexadecane-in-water emulsion is triggered by collisions involving solid particles. They performed experiments by means of nuclear magnetic resonance (NMR) spectroscopy to validate their hypothesis. Subcooled liquid droplets did not crystallize at a subcooling of 13 K even after 175 h. A mixture of 50 % liquid subcooled drops and 50 % solid particles showed a higher solid content after the same period. The droplet size distributions (Sauter diameter $x_{3,2}^{(1)} = 0.34\ \mu\text{m}$) were identical before and after the measurements. No external forces were induced during the experiments.

McClements, Dickinson, and Povey [17] found that an *n*-hexadecane-in-water emulsion inoculated with a solid *n*-hexadecane-crystal crystallized faster than the same emulsion inoculated with an *n*-octadecane crystal. Dickinson et al. [15] demonstrated by ultrasonic measurements that *n*-hexadecane-in-water emulsions ($x_{3,2} = 0.36\ \mu\text{m}$) consisting of a 1:1 mixture of liquid droplets and solid particles were completely crystallized after 500 h at $4\ ^\circ\text{C}$. Under the same conditions, even 100 % subcooled liquid droplets remained liquid after 500 h.

Especially for stirred emulsions, the flow type and, consequently, the interaction between liquid subcooled droplets and crystallized particles are of great importance (Fig. 1a). Although orthokinetic

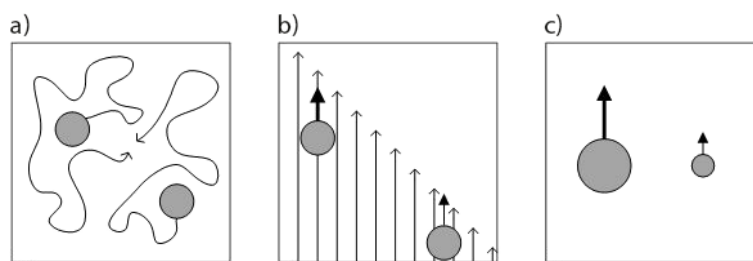


Figure 1. Three different causes for collisions of droplets and/or particles: (a) Brownian diffusion, (b) velocity gradient of the continuous phase, (c) difference in creaming velocities. Redrawn after [12].

movement is ubiquitous in technical approaches, the literature about this aspect is very limited [4, 9, 16]. The existing works show controversial results:

Povey et al. [9] detected an influence of stirring for *n*-hexadecane-in-water emulsions (emulsifier: Tween[®]20, $x_{3,2} = 130\text{--}2440\ \text{nm}$). The solid content increased more quickly in the stirred emulsion compared to the unstirred system. Flow velocities were not determined. Abramov et al. [4] published contradictory results about *n*-hexadecane-in-water dispersions. No crystallization could be observed at an average shear rate of $\dot{\gamma}_{\text{mean}} = 1250\ \text{s}^{-1}$ in a rotational rheometer, and the droplets remained liquid in the subcooled state.

Vanapalli and Coupland [16] postulated that the heterogeneous nucleation rate of an *n*-hexadecane-in-water emulsion (20 wt % *n*-hexadecane, 2 wt % Tween[®]20, $x_{3,2} = 0.3\ \mu\text{m}$) in the presence of solid *n*-hexadecane particles is independent of the shear rate at $6\ ^\circ\text{C}$. They utilized a self-constructed, concentric, and cylindrical rheometer for their measurements.

In accordance with literature [4, 9, 16], three outcomes are possible from a collision of a liquid droplet with a solid particle, i.e., a crystallized droplet of the same chemical composition as the liquid droplet (Fig. 2). Collisions leading to a nucleation of liquid droplets are called reactive in the following.

Consequently, not all the collisions are reactive and do not necessarily result in an increase of the solid fraction. Dickinson et al. reported as a result of their experiments that only

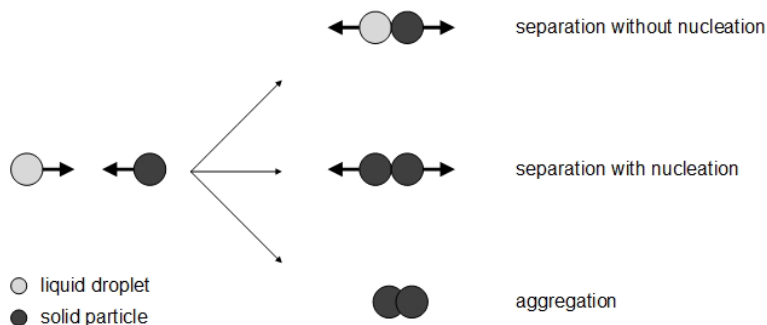


Figure 2. Possible results from the collision of a crystallized particle with a subcooled liquid droplet. Nucleation can take place or not during the contact of the two reaction partners. Additionally, partial coalescence and aggregation can occur.

1) List of symbols at the end of the paper.

one out of 10^7 collisions led to a nucleation of the liquid droplet [15].

There is great potential in more precise knowledge about the influence of flow fields on the solid content of the dispersion phase since the production and storage of industrial emulsions is of tremendous significance. In this work, a Taylor-Couette geometry was constructed and integrated into an NMR spectrometer to determine the influence of the flow field on the crystallization behavior and crystallization kinetics of an *n*-hexadecane-in-water emulsion in-line and in a non-invasive way. The aim of this work was to verify that (i) collision-induced crystallization occurs during crystallization of organic emulsions exposed to different shear rates, and that (ii) an increased shear rate leads to a rise in the collision rate, resulting in a larger number of reactive collisions within the emulsion.

Within this work, the influence of shear flow on the crystallization of molten *n*-hexadecane droplets in oil-in-water emulsions was investigated. Therefore, a Rheo-NMR setup had to be constructed and evaluated. The following parts will deal, firstly, with the necessary theory, followed by the construction and validation of the measurement setup. Finally, the experimental results and a corresponding discussion are presented.

2 Theory

2.1 Calculation of the Collision Frequency

The volume-specific collision rate of droplets and particles with the diameters x_L and x_S is described by the collision rate h_{coll} :

$$h_{\text{coll}}(x_S, x_L) = n_S n_L \beta_{\text{SL}} \quad (1)$$

Where n_L and n_S are the number densities of liquid droplet and crystalline particle classes with sizes x_L and x_S ; β_{SL} corresponds to the collision kernel, which can be determined for laminar flow, turbulent flow, and the transition region. Only the influence of laminar flow on the collision frequency is of interest for this work, since laminar flow is the only flow regime. According to Smoluchowski [18], the collision kernel for laminar flow may be calculated as a function of the shear rate:

$$\beta_{\text{SL, lam}} = \frac{4}{3} \dot{\gamma} \left(\frac{x_S}{2} + \frac{x_L}{2} \right)^3 \quad (2)$$

Droplets and particles can also move by Brownian motion, also called Brownian diffusion. Brownian diffusion for droplets and particles with a diameter larger than $1 \mu\text{m}$ can be neglected compared to collisions due to the velocity gradient of the continuous phase. This is the case in the present work since the emulsions used have an average droplet diameter of $x_{50,3} = 2.8\text{--}4.0 \mu\text{m}$. Moreover, Brownian diffusion does not have to be considered for Péclet numbers greater than 1 [19]. The Péclet number is defined as:

$$Pe = \eta \dot{\gamma} \frac{\left(\frac{x}{2}\right)^3}{k_B T} \quad (3)$$

It describes the ratio of the forces acting on the particles as a result of the displacement caused by external fluid movement and diffusion. The Péclet number for the measurement setup and parameters used was calculated at above 40.

2.2 Further Descriptions of the Crystallization Process

The fraction of crystallized droplets ξ at time t can be expressed by a second order kinetics (e.g. [15]):

$$\frac{d(1 - \xi)}{dt} = -k_{\text{coll}} \xi (1 - \xi_0) \quad (4)$$

Where k_{coll} represents a second-order kinetic constant. As soon as crystallization occurred due to a reactive collision, it was assumed that, in addition to the inoculated particles, the newly formed particles can cause nucleation with the same reactivity.

The fraction of crystallized droplets $\xi(t)$ is defined as the ratio of the number of crystallized droplets at time t to the number of liquid droplets at time t_0 :

$$\xi(t) = \frac{n_S(t)}{n_L(t_0)} \quad (5)$$

Dickinson et al. [15] used Eq. (4) to describe the crystallization in an emulsion which consisted initially of 50 % solid particles and 50 % liquid droplets. They postulated that nucleation is triggered by processes associated with the free emulsifier concentration in the continuous phase since no flow field was applied to the emulsion. They determined values k_{coll} between 1.7×10^{-6} and $9.2 \times 10^{-6} \text{ s}^{-1}$ for different free emulsifier concentrations of Tween®20 ($6\text{--}63 \text{ mol m}^{-3}$). A second-order approach was also employed by McClements et al. [14, 17].

Using a population balance for the dispersion, the change of the number density of solid particles can be calculated by:

$$\begin{aligned} \frac{\partial n_S}{\partial t} &= J_{\text{sec}} = \lambda_{\text{sec}} h_{\text{coll}} = \lambda_{\text{sec}} \beta_{\text{SL}} n_L n_S \\ &= \lambda_{\text{sec}} \beta_{\text{SL}} n_{\text{total}}^2 \xi (1 - \xi) = n_{\text{total}} \frac{\partial \xi}{\partial t} \end{aligned} \quad (6)$$

Where J_{sec} describes the nucleation rate of liquid droplets. As not all collisions lead to nucleation, a nucleation efficiency λ_{sec} is introduced. If all collisions would lead to crystallization, the nucleation efficiency is 1. n_{total} represents the number density of all liquid and solid droplets/particles and as the disperse phase is constant during the experiments, n_{total} is the same as $n_L(t_0)$.

Comparing Eq. (4) and Eq. (6) leads to:

$$k_{\text{coll}} = \lambda_{\text{sec}} \beta_{\text{SL}} n_{\text{total}} \quad (7)$$

3 Materials and Methods

3.1 Materials

The emulsions consisted of 78 wt % ultrapure water (resistance: 18.2 M Ω cm, Sigma-Aldrich), 20 wt % *n*-hexadecane (purity > 99.0 %, Carl Roth, bulk crystallization temperature $T_S = 296.15$ K) and 2 wt % polysorbate 20 (trading name: Tween[®] 20, Carl Roth). *N*-Hexadecane was dispersed in water using a gear rim dispersing machine (IKA[®] T25 digital, 5 min, 20 000 rpm). An emulsion with reproducible droplet size distribution (DSD) between 1 and 10 μ m was produced (Fig. 4, black curve). Thus, the oil-in-water emulsion has a continuous phase with ultrapure water and *n*-hexadecane as the disperse phase, which was stabilized by Tween[®] 20 as emulsifier.

3.2 Methods

All spectroscopic and diffusion NMR measurements were performed on a 400-MHz NMR spectrometer (AvI; Bruker Bio-Spin GmbH; probe: Diff30, 10 mm max. sample diameter). NMR was chosen as measurement method due to the ability to acquire experimental data online during crystallization and due to its non-invasiveness. Furthermore, NMR offers the opportunity to determine the emulsifiers' behavior and the droplet size distribution by means of diffusion measurements during crystallization as well.

¹H NMR spectra were recorded every minute. The fraction of crystallized particles was quantified by integration of the *n*-hexadecane peaks (CH₃ and CH₂). The Rheo-NMR measurement setup [20], temperature profile, and determination of solid fraction according to the NMR spectra can be found in the Supporting Information.

4 Results and Discussion

Mean shear rates of 0, 148, 222, and 296 s⁻¹ were realized to quantify the influence of shear rates on crystallization. The amount of solid *n*-hexadecane which was produced during the time of rotation increases with rising shear rates (Fig. 3).

A slight increase of the fraction of crystallized *n*-hexadecane droplets was detectable at 0 s⁻¹ and 6 K subcooling during the measurement (Fig. 3, grey symbols). It is assumed that this observation results from droplets moving past each other due to creaming.

According to Stokes' law [21], *n*-hexadecane droplets with a diameter of 2.8 μ m move with a velocity of 8.8 $\times 10^{-6}$ ms⁻¹ through the continuous water phase. The droplets were able to move a maximum of 2.8 mm within the total experimental time of 2700 s = 0.75 h (Fig. 3). The measurement height, i.e., the sensitive region of the NMR probe, is about 2 cm. Thus, any phase separation due to creaming can be neglected on that time scale. Moreover, the integral of the water peak in the NMR spectra during the experiments' duration did not show any relevant creaming effects of the emulsion. If creaming occurred, the integral of the water peak would increase additionally to a decrease of the *n*-hexadecane integral, indicating that the drop-

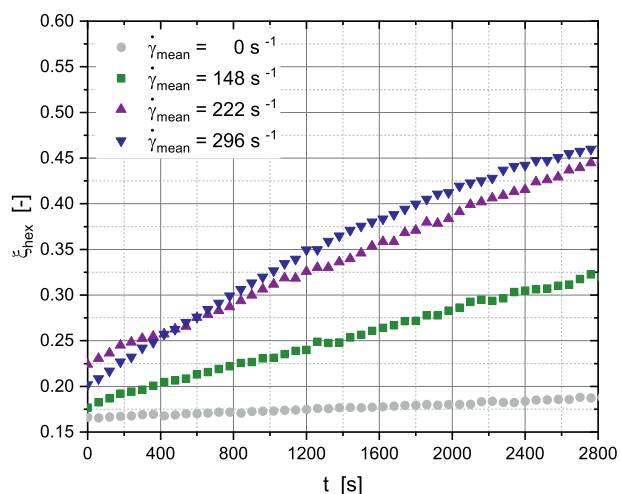


Figure 3. Solid fraction of *n*-hexadecane as a function of time for different shear rates at $\Delta T = 6$ K.

lets would have left the measurement range due to creaming. Only the *n*-hexadecane area integral decreased in the experiments, but no changes of the water integral were noticeable. Thus, only crystallization of *n*-hexadecane happened and no creaming of the emulsion was observed on the mentioned time scale.

According to Walstra [22], the droplets are too inert to deform or even break up in a simple laminar shear flow for viscosity ratios of the dispersed to the continuous phase ($\eta_D \eta_C^{-1}$) larger than 4. Thus, the Weber number does not exceed the critical Weber number.

One could argue that the observations in Fig. 3 are due to changes in droplet size distribution which might change during rotation owing to shear forces. Therefore, diffusion NMR measurements were performed to justify the negligibility of a possible influence of shear stress and storage on the DSD (Fig. 4). The differences found in the DSD are within measurement tolerances.

To model the data in Fig. 3, a second-order kinetics was used to calculate the collision-induced secondary nucleation (Eq. (4)). The model considers the interaction of a reactive pair consisting of a liquid droplet and a solid particle.

The fraction of crystallized *n*-hexadecane droplets increases with shear rate in the time interval shown (Fig. 3) as does the kinetic constant k_{coll} . Tab. 1 summarizes the values determined for the initial solid content of *n*-hexadecane $\xi_{0,\text{fit}}$, the kinetic constants k_{coll} according to the fit of Eq. (4) to the data, and the solid content of *n*-hexadecane ξ_0 measured, determined by evaluating the NMR spectra.

An agreement between the calculated and fitted values was found for the solids fraction at the time $t = 0$ h when the rotation was started. This indicates that the selected model reproduces the crystallization kinetics in the shear field well without primary nucleation influences such as temperature.

The kinetic constant k_{coll} increases linearly with the mean shear rate for the values measured with a slope of 1.3×10^{-6} (Fig. 5).

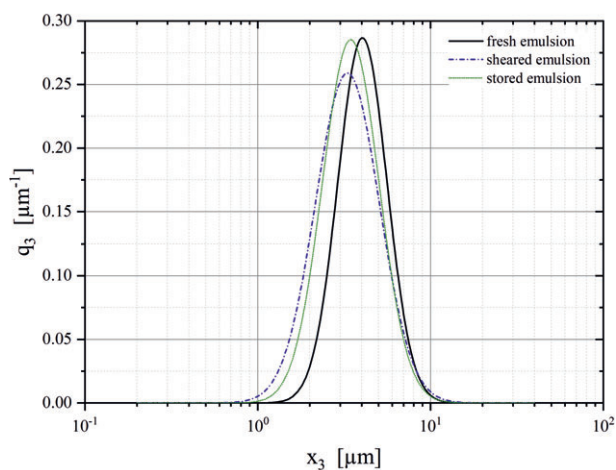


Figure 4. q_3 -droplet size distributions of an *n*-hexadecane-in-water emulsion measured by means of pulsed field gradient NMR diffusion measurements ($\Delta = 0.1$ s, $\delta = 2 \times 10^{-3}$ s). Different droplet size distributions are visible for a fresh, a stored, and a sheared emulsion. The difference between the fresh and the sheared emulsion is within the tolerances expected. Fresh emulsion: $x_{50,3} = 4.0$ μm , sheared emulsion: $x_{50,3} = 3.3$ μm , stored emulsion: $x_{50,3} = 3.8$ μm .

Table 1. Kinetic constant (k_{coll}), calculated fraction of crystallized *n*-hexadecane droplets at the beginning of shear ($\xi_{0,\text{fit}}$), and the solid fractions of *n*-hexadecane determined from the NMR spectra (ξ_0) for the different shear rates.

	Shear rates $\dot{\gamma}_{\text{mean}}$ [s^{-1}]			
	0	148	222	296
k_{coll} [s^{-1}]	5.2×10^{-5}	2.7×10^{-4}	3.6×10^{-4}	4.3×10^{-4}
$\xi_{0,\text{fit}}$ [-]	0.17	0.19	0.23	0.23
ξ_0 [-]	0.17	0.18	0.22	0.20

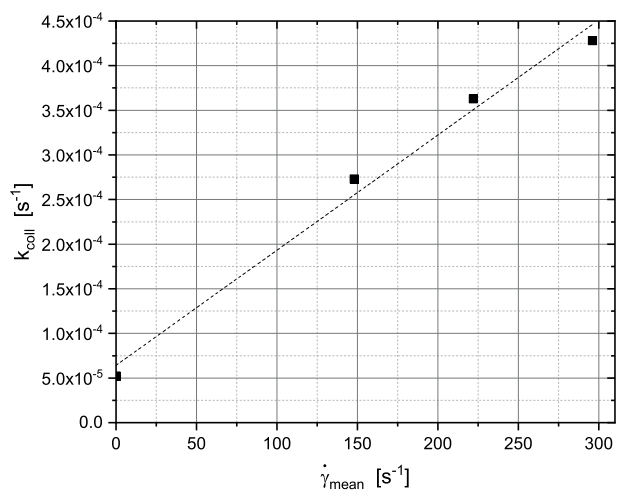


Figure 5. Relation between kinetic constant k_{coll} and shear rate $\dot{\gamma}_{\text{mean}}$. A linear relation between k_{coll} and $\dot{\gamma}_{\text{mean}}$ was observed.

Dickinson et al. [15] used a second-order kinetic to describe the crystallization process of an emulsion which consisted initially of 50% solid particles and 50% liquid droplets. They postulated that nucleation arises due to processes associated with the free emulsifier concentration in the continuous phase since no external shear forces acted on the emulsion. They determined values for k_{coll} between $1.7 \times 10^{-6} \text{ s}^{-1}$ and $9.2 \times 10^{-6} \text{ s}^{-1}$ for different free emulsifier concentrations of Tween[®]20 ($6\text{--}63 \text{ mol m}^{-3}$). A second-order approach was also applied by McClements et al. [14, 17]. With no external shear stress and an initial solid content of 17%, $k_{\text{coll}} = 5.2 \times 10^{-5} \text{ s}^{-1}$ in the experiments.

A statement can be found in the literature that one of 10^7 collisions in an *n*-hexadecane-in-water dispersion leads to crystallization [15]. Based on the number density of *n*-hexadecane droplets in the NMR sensitive emulsions' volume (total number of droplets $N_{\text{total}} = 2.9 \times 10^9$) and the average shear rate, the nucleation efficiency λ_{sec} was calculated by Eq. (7). An average droplet and particle size of $2.8 \mu\text{m}$ was assumed for the calculation.

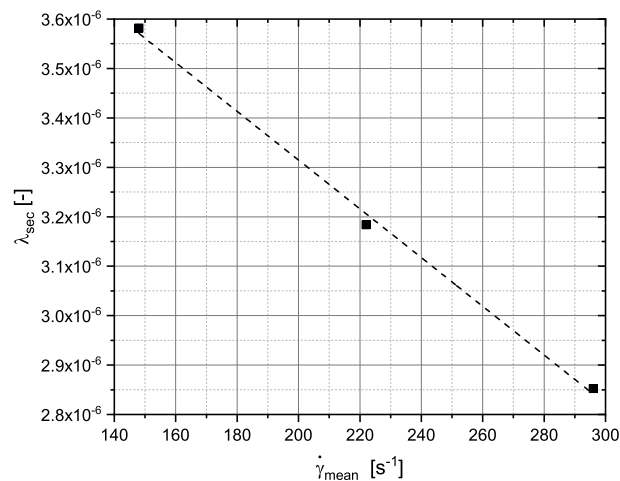


Figure 6. Nucleation efficiency λ_{sec} as a function of the mean shear rate, calculated according to Eq. (7) with an average droplet/particle size of $2.8 \mu\text{m}$. The line describes a linear fit with $\lambda_{\text{sec}} = 4.3 \times 10^{-6} \text{ s } \dot{\gamma}_{\text{mean}} - 4.9 \times 10^{-5}$.

About one out of 3×10^5 collisions was reactive during the experiments. The nucleation efficiency of the collisions decreased slightly from 3.6×10^{-6} at $\dot{\gamma}_{\text{mean}} = 148 \text{ s}^{-1}$ to 2.9×10^{-6} at $\dot{\gamma}_{\text{mean}} = 296 \text{ s}^{-1}$. Therefore, it can be stated that the increase of the shear rate and, thus, a higher flow velocity but a shorter contact time resulted in a reduction of the nucleation efficiency. This leads to the assumption that the flow field and shear rate applied cannot improve the efficiency, but the contact time is probably the parameter of interest. Using Levich's approach [23] for stirred dispersions, the contact time is proportional to the square root of the energy dissipation. As the square root of the energy dissipation is proportional to the shear rate, the contact time decreases as the shear rate increases. Nevertheless, a higher shear rate resulted in a sharper increment of the solid content.

Dickinson et al. [15] used an *n*-hexadecane-in-water emulsion with a different DSD for their measurements (in this work: $x_{50.3} = 2.8\text{--}4.0\ \mu\text{m}$, in their work: $0.32\text{--}0.37\ \mu\text{m}$). The discrepancy between the literature value and the number of reactive collisions calculated in this study can be explained by the difference in DSD of the two emulsions and the shear rates applied in this work. Furthermore, the concentrations of the emulsifier Tween[®]20 differ, as do the disperse phase fraction of *n*-hexadecane and the process temperature. These differences have an influence on the reactivity of the collisions since crystallization by collision of droplets and particles depends on the following factors: process temperature (and, thus, the subcooling of the substance to be crystallized), DSD, type and concentration of the disperse phase, continuous phase, and emulsifier [17,24].

5 Conclusion

The influence of laminar shear flow on the crystallization of an *n*-hexadecane-in-water emulsion was investigated. A Rheo-NMR apparatus was realized and a method for the measurement of the impact of applied flow rates was developed. In the first step, a Taylor-Couette geometry, which allowed the liquid fraction of *n*-hexadecane to be measured using a 400-MHz NMR spectrometer, was built and put into operation [20]. Pulsed-field gradient NMR also enabled the in-line and non-destructive determination of the droplet size distribution of the emulsion.

The crystallization kinetics of the *n*-hexadecane-in-water emulsion was analyzed for shear rates up to $\dot{\gamma}_{\text{mean}} = 296\ \text{s}^{-1}$. A second-order kinetics was employed for the modeling of the solid content of *n*-hexadecane, and the corresponding kinetic constants were determined. An increase in shear rate and, thus, in flow velocity resulted in a faster crystallization, which was reflected in a higher kinetic constant and a higher number of reactive collisions per second.

The study indicated that one of about 3×10^5 collisions of a crystalline particle with a liquid droplet led to crystallization of the droplet. The collision efficiency was the highest (3.6×10^{-6}) for a shear rate of $\dot{\gamma}_{\text{mean}} = 148\ \text{s}^{-1}$. The solid fraction of *n*-hexadecane at the beginning of the rotation corresponded to the initial solid fractions, which were determined by means of integration of the NMR spectra, with a maximum deviation of 10 %, showing a good agreement of the second-order kinetics chosen with the experimental data.

Following the coalescence theory [25], three external factors can influence the collision efficiency: the collision frequency, the contact force, and the contact time. As the collision frequency increases and the contact time decreases with the shear rate, these are opposing effects. In further work, the relation between these influencing factors on the crystallization kinetics will be evaluated.

Supporting Information

Supporting Information for this article can be found under DOI: <https://doi.org/10.1002/ceat.202000193>.

Acknowledgment

The authors thank the Bruker BioSpin GmbH, μ -imaging group, for their support during this work. The financial support by the Arbeitsgemeinschaft industrieller Forschungsvereinigungen (project No.19682 N) is gratefully acknowledged. The Deutsche Forschungsgesellschaft is thanked for the substantial financial contribution in form of NMR instrumentation and within the instrumental facility Pro²NMR. The authors also would like to acknowledge the workshop employees for their support during the constructions.

The authors have declared no conflict of interest.

Symbols used

h_{coll}	$[\text{m}^{-3}\text{s}^{-1}]$	volume-specific collision rate
J_{sec}	$[\text{m}^{-3}\text{s}^{-1}]$	nucleation rate
K_{B}	$[\text{m}^2\text{kg s}^{-2}\text{K}^{-1}]$	Boltzmann's constant
k_{coll}	$[\text{s}^{-1}]$	second order kinetic constant
n_{L}	$[\text{m}^{-3}]$	number density of liquid droplets
n_{S}	$[\text{m}^{-3}]$	number density of solid particles
n_{total}	$[\text{m}^{-3}]$	total number density of solid particles and liquid droplets
N_{total}	$[-]$	total amount of droplets
t	$[\text{s}]$	time
t_0	$[\text{s}]$	time when rotation started
T	$[\text{K}]$	temperature
T_{S}	$[\text{K}]$	bulk crystallization temperature
x	$[\mu\text{m}]$	droplet/particle diameter
$x_{3.2}$	$[\mu\text{m}]$	Sauter diameter
$x_{50.3}$	$[\mu\text{m}]$	volumetric mean droplet diameter
x_{L}	$[\mu\text{m}]$	diameter of liquid droplets
x_{S}	$[\mu\text{m}]$	diameter of solid particles

Greek letters

β_{SL}	$[\text{m}^3\text{s}^{-1}]$	collision kernel of solid particle and liquid droplet
$\beta_{\text{SL,lam}}$	$[\text{m}^3\text{s}^{-1}]$	collision kernel of solid particle and liquid droplet for laminar flow
ΔT	$[\text{K}]$	subcooling
Δ	$[\text{s}]$	diffusion time
δ	$[\text{s}]$	duration of the magnetic field gradient pulse
η	$[\text{kg m}^{-1}\text{s}^{-1}]$	dynamic viscosity
η_{C}	$[\text{kg m}^{-1}\text{s}^{-1}]$	dynamic viscosity of continuous phase
η_{D}	$[\text{kg m}^{-1}\text{s}^{-1}]$	dynamic viscosity of dispersed phase
$\dot{\gamma}$	$[\text{s}^{-1}]$	shear rate
$\dot{\gamma}_{\text{mean}}$	$[\text{s}^{-1}]$	mean shear rate
λ_{sec}	$[-]$	nucleation efficiency
ξ	$[-]$	fraction of solid particles
ξ_0	$[-]$	fraction of solid particles when rotation started
$\xi_{0,\text{fit}}$	$[-]$	fraction of solid particles when rotation started according to the fit

Abbreviations

DSD	droplet size distribution
NMR	nuclear magnetic resonance

References

- [1] J. Pardeike, A. Hommoss, R. H. Müller, *Int. J. Pharm.* **2009**, *366* (1–2), 170–184. DOI: <https://doi.org/10.1016/j.ijpharm.2008.10.003>
- [2] S. A. Wissing, R. H. Müller, *Int. J. Pharm.* **2003**, *254* (1), 65–68. DOI: [https://doi.org/10.1016/s0378-5173\(02\)00684-1](https://doi.org/10.1016/s0378-5173(02)00684-1)
- [3] D. J. McClements, *Adv. Colloid Interface Sci.* **2012**, *174*, 1–30. DOI: <https://doi.org/10.1016/j.cis.2012.03.002>
- [4] S. Abramov, A. Berndt, K. Georgieva, P. Ruppik, H. P. Schuchmann, *Colloids Surf., A* **2017**, *529*, 513–522. DOI: <https://doi.org/10.1016/j.colsurfa.2017.06.029>
- [5] J. N. Coupland, *Curr. Opin. Colloid Interface Sci.* **2002**, *7* (5), 445–450. DOI: [https://doi.org/10.1016/S1359-0294\(02\)00080-8](https://doi.org/10.1016/S1359-0294(02)00080-8)
- [6] P. Walstra, *Physical Chemistry of Foods*, Food Science and Technology, Vol. 121, Marcel Dekker, New York **2003**.
- [7] M. J. W. Povey, *Food Hydrocolloids* **2014**, 42118–42129. DOI: <https://doi.org/10.1016/j.foodhyd.2014.01.016>
- [8] I. Gülseren, J. N. Coupland, *Cryst. Growth Des.* **2007**, *7* (5), 912–918. DOI: <https://doi.org/10.1021/cg060683f>
- [9] M. J. W. Povey, T. S. Awad, R. Huo, Y. Ding, *Eur. J. Lipid Sci. Technol.* **2009**, *111* (3), 236–242. DOI: <https://doi.org/10.1002/ejlt.200800193>
- [10] R. W. Hartel, *Crystallization in Foods*, Aspen Food Engineering Series, Aspen Publ., Gaithersburg, MD **2001**.
- [11] B. Spiegel, A. Käfer, M. Kind, *Cryst Growth Des.* **2018**, *18* (6), 3307–3316. DOI: <https://doi.org/10.1021/acs.cgd.7b01697>
- [12] *Food Emulsions*, 4th ed. (Eds.: S. Friberg, K. Larsson, J. Sjöblom), Food Science and Technology, Marcel Dekker, New York **2004**.
- [13] G. M. Pound, V. K. La Mer, *J. Am. Chem. Soc.* **1952**, *74* (9), 2323–2332. DOI: <https://doi.org/10.1021/ja01129a044>
- [14] D. J. McClements, S. R. Dungan, *J. Colloid Interface Sci.* **1997**, *186* (1), 17–28.
- [15] E. Dickinson, F.-J. Kruijenga, J. W. Povey, M. van der Molen, *Colloids Surf., A* **1993**, 81273–81279. DOI: [https://doi.org/10.1016/0927-7757\(93\)80255-D](https://doi.org/10.1016/0927-7757(93)80255-D)
- [16] S. A. Vanapalli, J. N. Coupland, *Food Hydrocolloids* **2001**, *15* (4–6), 507–512. DOI: [https://doi.org/10.1016/S0268-005X\(01\)00057-1](https://doi.org/10.1016/S0268-005X(01)00057-1)
- [17] J. D. McClements, E. Dickinson, J. W. M. Povey, *Chem. Phys. Lett.* **1990**, *172* (6), 449–452. DOI: [https://doi.org/10.1016/0009-2614\(90\)80137-3](https://doi.org/10.1016/0009-2614(90)80137-3)
- [18] M. v. Smoluchowski, *Z. Phys. Chem. (N F)* **1918**, *92U* (1). DOI: <https://doi.org/10.1515/zpch-1918-9209>
- [19] H. A. Barnes, *Colloids Surf., A* **1994**, *91*, 89–95. DOI: [https://doi.org/10.1016/0927-7757\(93\)02719-U](https://doi.org/10.1016/0927-7757(93)02719-U)
- [20] D. Morimoto, E. Walinda, N. Iwakawa, M. Nishizawa, Y. Kawata, A. Yamamoto, M. Shirakawa, U. Scheler, K. Sugase, *Anal. Chem.* **2017**, *89* (14), 7286–7290. DOI: <https://doi.org/10.1021/acs.analchem.7b01816>
- [21] G. G. Stokes, *Trans. Camb. Philos. Soc.* **1851**, *9*, 8–106.
- [22] P. Walstra, *Chem. Eng. Sci.* **1993**, *48* (2), 333–349. DOI: [https://doi.org/10.1016/0009-2509\(93\)80021-H](https://doi.org/10.1016/0009-2509(93)80021-H)
- [23] C. A. Coulaloglou, L. L. Tavlarides, *Chem. Eng. Sci.* **1977**, *32* (11), 1289–1297. DOI: [https://doi.org/10.1016/0009-2509\(77\)85023-9](https://doi.org/10.1016/0009-2509(77)85023-9)
- [24] O. I. Mikhalev, I. N. Karpov, E. B. Kazarova, M. V. Alfimov, *Chem. Phys. Lett.* **1989**, *164* (1), 96–100. DOI: [https://doi.org/10.1016/0009-2614\(89\)85209-1](https://doi.org/10.1016/0009-2614(89)85209-1)
- [25] A. K. Chester, *Chem. Eng. Res. Des.* **1991**, *69* (A4), 259–270.
- [26] C. D. Andereck, S. S. Liu, H. L. Swinney, *J. Fluid Mech.* **1986**, *164* (1), 155. DOI: <https://doi.org/10.1017/S0022112086002513>

Research Article: Collision-induced nucleation was utilized to accelerate crystallization kinetics, avoiding energetically unfavorable low process temperatures. An increase of crystallization rate with shear rate, yielding higher final solid fractions, was determined. Not every solid-liquid contact results in the crystallization of the liquid droplet, as the collision efficiency decreased with increasing shear rate.

Influence of Shear Flow on the Crystallization of Organic Melt Emulsions – A Rheo-Nuclear Magnetic Resonance Investigation

G. Kaysan, B. Spiegel, G. Guthausen, M. Kind*

Chem. Eng. Technol. **2020**, *43* (XX), XXX ... XXX

DOI: 10.1002/ceat.202000193



Supporting Information
available online

